J Fluoresc (2013) 23:357–366
DOI 10.1007/s10895-013-1157-2

FLUORESCENCE NEWS ARTICLE

Oxygen Diffusion into Multiwalled Carbon Nanotube Doped Polystrene Latex Films Using Fluorescence Technique

Önder Yargı · Şaziye Uğur · Önder Pekcan

Received: 6 August 2012 / Accepted: 7 January 2013 / Published online: 19 January 2013

Abstract This study examines the oxygen diffusion into polystyrene (PS) latex/multiwalled carbon nanotube (MWNT) nanocomposite films (PS/MWNT) consisting of various amounts of MWNT via steady state fluorescence technique (SSF). PS/MWNT films were prepared from the mixture of MWNT and pyrene (P)-labeled PS latexes at various compositions at room temperature. These films were then annealed at 170 °C above glass transition (T_g) temperature of PS. Fluorescence quenching measurements were performed for each film separately to evaluate the effect of MWNT content on oxygen diffusion. The Stern-Volmer equation for fluorescence quenching is combined with Fick's law for diffusion to derive the mathematical expressions. Diffusion coefficients (D) were produced and found to be increased from 1.1×10^{-12} to 41×10^{-12} cm^2s^{-1} with increasing MWNT content. This increase was explained via the existence of large amounts of pores in composite films which facilitate oxygen penetration into the structure.

Keywords Carbon nanotubes · Fluorescence · Diffusion · Oxygen · Quenching · Composite film

Introduction

In the last few years, the use of polymers as coating materials for the protection of the active ingredient of solid pharmaceutical products against decomposition due to environmental conditions has been greatly increased. Apart from acting as a moisture barrier or controlling the release of the active agent, the most desirable property of these polymer films is their resistance to the gas diffusion. Because single component polymer films have poor mechanical and gas barrier properties, there has been growing interest in producing new materials by filling polymers with inorganic natural (minerals) and/or synthetic (carbon black and silica) compounds[1–5]. They give improved mechanical properties, gas barrier properties, and decreased flammability relative to the simple polymers [6]. In 2000, the potential for CNTs as gas sensors was first reported based on an increase in the conductivity by several orders of magnitude upon exposure of CNTs to oxygen [7]. Oxygen is the one of the most important reactants to be considered in the diffusion phenomenon. The control of the diffusion of oxygen is of particular importance in polymer oxidative degradation, protective coatings, and in the design of polymeric membranes for separation processes in production of films for packing industry, and in the developments of biocompatible materials. These results were subsequently questioned [8]. The enhancement in barrier properties in composites depends on several factors, such as the amount, length, and width of the filler, orientation and dispersion of the filler particles.

For more than fifty years, polymer scientists have been interested in the influence of fillers on gas diffusion through polymer membrane [9–13]. This analysis provides us important knowledge about the effect of mineral fillers on the performance of oxygen sensors. Gorrasi et al.[14] studied the transport properties of *n*-pentane and dichloromethane vapors in polypropylene–organophilic layered silicates nanocomposites with different clay concentration. It was found that the permeability of both solvent vapors was reduced, mainly due to the decreased diffusion, since the solubility was less affected by the presence of fillers. Lu et al. [11] examined the influence of 10 nm diameter silica particles on oxygen diffusion in PDMS polymer film. A

Ö. Yargı
Department of Physics, Yildiz Technical University,
Esenler 34210 Istanbul, Turkey

Ş. Uğur (✉)
Department of Physics, Istanbul Technical University,
Maslak 34469 Istanbul, Turkey
e-mail: saziye@itu.edu.tr

Ö. Pekcan
Faculty of Science and Arts, Kadir Has University, Cibali 34320
Istanbul, Turkey

decrease was observed in oxygen diffusion coefficients, D with increasing silica content. This reduction in D was attributed to the tortuous path towards diffusing gas molecules and reduced molecular mobility of polymer chains caused by the filler particles.

Oxygen diffusivity in polymers is most commonly determined by measuring the rate of oxygen permeation across a membrane. One exposes one side of the polymer film to oxygen at time zero and measures the flux of oxygen across the film as a function of time. Knowing the dimensions of the film and the partial pressure of oxygen on the high-pressure side, one can calculate the diffusion coefficient from the flux [15]. The diffusion coefficient of oxygen is determined from the kinetics of the approach of the oxygen, flux to its steady-state. Because oxygen is such a powerful quencher of fluorescence and phosphorescence, there is a natural attraction to using this property to determine this value. Another approach due to Cox also looks at large samples [16]. Here one constructs a square cell with centimeter-scale height. The cell is filled with a polymer containing the dye and all oxygen is removed. Cox irradiated a thin (1 mm) middle cross section of the cell, and then allowed oxygen to diffuse into the cell from the top. As the oxygen concentration profile propagates through the illuminated middle slice, the emission intensity is quenched.

Several spectroscopic techniques that utilize oxygen quenching to determine the rate of oxygen diffusion through polymer films have been reported. The luminescence quenching by oxygen was applied to the study of oxygen diffusion properties in polymers [17–27]. For measuring diffusion coefficients of oxygen in polymers using luminescence quenching methods, a fluorophore is typically dispersed directly in the polymer, and the change in the average oxygen concentration is monitored by studying the average intensity change or lifetime change of the a fluorophore using a spectrofluorometer [17–27]. In these methods, the polymer is initially equilibrated at a particular concentration of oxygen and then, the polymer containing a fluorophore is exposed to oxygen. The average intensity or lifetime change in the polymer is monitored using a spectrofluorometer for determining diffusion coefficients. The diffusion coefficient of oxygen into Poly (methyl methacrylate) (PMMA) was determined by the quenching of phosphorescence of phenanthrene added into polymer [17]. Barker has utilized the bleaching action of oxygen on color centers produced by electron beam irradiation of polycarbonate and PMMA by following optically the moving boundary [18]. The quenching of fluorescence of naphthalene in PMMA was studied by oxygen in thin films after displacement of nitrogen atmosphere over the sample by oxygen [19]. Cox [20] and Dunn [21], MacCallum and Rudkin [22] measured oxygen diffusion coefficient by fluorescence quenching in planar sheets of poly (dimethyl siloxane) [20], filled poly (dimethyl siloxane) sample [21] and polystyrene [22]. They monitored oxygen quenching of a fluorophore as a function of time by assuming that fluorophore dispersed homogeneously within the films. The mathematical determination of D varied, but a single underlying assumption in all cases was that the time-dependent emission intensity measured during the experiment. In some cases, the intensity versus time curve was converted to a concentration versus time curve using the Stern-Volmer relationship [20, 21]. Winnik and Manners [23–25] have used time-scan experiments to measure the decay of luminescence intensity as oxygen diffuses into polymer films under constant illumination and the growth of intensity as oxygen diffuses out of the film. They interpreted their data with the aid of theoretical expressions based on Stern-Volmer quenching kinetics with Fick's laws of diffusion. In some of our earlier studies, we examined the effect of annealing [26] and packing [27] on the oxygen diffusion coefficient, D, in poly(methyl methacrylate) by using steady state (SSF) and photon transmission (PT) techniques.

In the present work, we used a technique based on fluorescence quenching to investigate oxygen diffusion behavior in PS/MWNT nanocomposite films containing various amount of MWNT. Initially, PS/MWNT composite films were equilibrated at a particular oxygen concentration and then after displacement of nitrogen atmosphere over the sample by oxygen, the film began to exposed to lower oxygen concentration. Since fluorescence intensity is proportional to the concentration of oxygen, the average oxygen concentration in the film sample was detected by monitoring the change in fluorescence intensity using a spectrofluorometer. We assume the quenching is accurately described by a linear Stern-Volmer equation and the optical density is low enough that the sample is uniformly excited. We combined the Stern-Volmer equation with Fick's law of diffusion to extract the diffusion coefficients from experimental data.

Experimental

Materials

Pyrene (P)-labelled polystyrene (PS) particles were produced via the emulsifier-free radical polymerization process [28]. The polymerization was carried out in a 200-ml thermostated round-bottomed four-necked flask, equipped with a glass anchor stirrer, reflux condenser and nitrogen inlet. Styrene monomer (commercial) was introduced in the reactor containing boiled and deionised water and the fluorescent monomer pyren-1-ylmethyl methacrylate (PolyFluorTM394) was first dissolved in a small amount of styrene. The potassium persulfate (KPS) initiator was dissolved in water and added when the polymerization temperature was equilibrated at 70°C. The stirring rate was 400 rpm. The recipe for the prepared latex is as follows: 100 ml water, 5 g of styrene, 0.1 g of KPS

(dissolved in 2 ml water) and 0.0129 g of fluorescent monomer (dissolved in 1 g styrene). The polymerization was conducted during 18 h under nitrogen atmosphere. The particles obtained are spherical and fairly monodisperse, all having very similar mean diameters (400 nm). The glass transition temperatures (T_g) of the PS latexes were determined using a differential scanning calorimeter (DSC) and found to be around 105 °C. The latex dispersion has an average particle size of 400 nm. Fig. 1a shows SEM image of PS latex produced for this study.

Commercially available MWNTs (Cheap Tubes Inc., VT, USA, 10–30 μm long, average inner diameter 5–10 nm, outer diameter 20–30 nm, the density is approximately 2.1 g/cm^3 and purity higher than 95 wt %) were used as supplied in black powder form without further purification. A stock solution of MWNTs was prepared following the manufacturers regulations: nanotubes were dispersed in deionized (DI) water with the aid of Polyvinyl Pyrolidone (PVP) in the proportions of 10 parts MWNTs; 1–2 parts PVP; 2.000 parts DI water by bath sonication for 3 h. PVP is a good stabilizing agent for dispersions of carbon nanotubes, enabling preparation of polystyrene composites from dispersions of MWNT in polystyrene solution. Figure 1b shows the TEM image of MWNTs used in this study (www.cheaptubesinc.com).

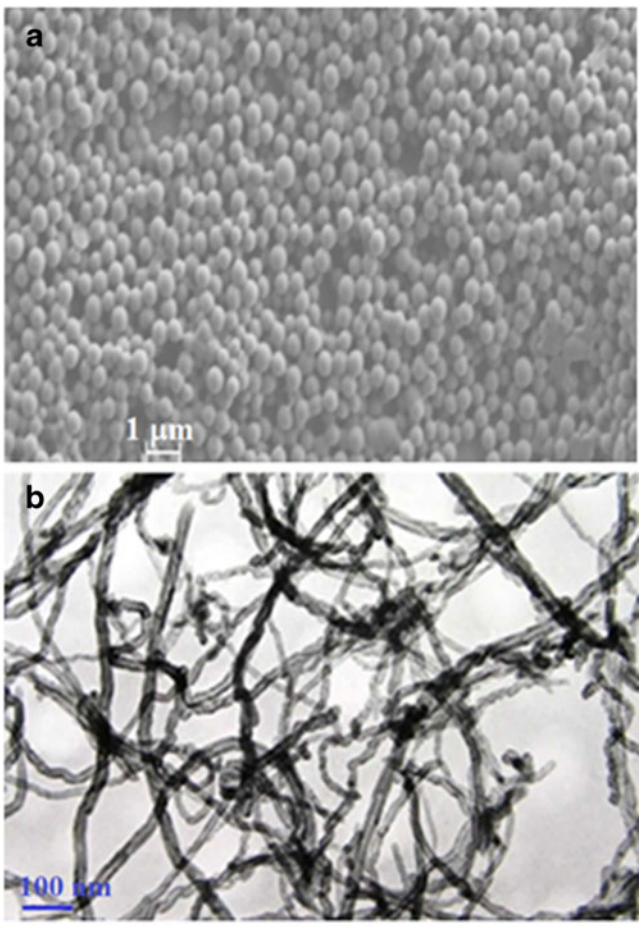

Fig. 1 **a** SEM picture of pure PS latex. **b** TEM picture of MWNT

PS/MWNT Composite Films

A 15 g/L solution of polystyrene (PS) in water was prepared separately. The dispersion of MWNT in water was mixed with the solution of PS yielding the required proportion of nanotubes and PS latex by using the relation:

$$R = \frac{M_{MWNT}}{M_{PS} + M_{MWNT}} \quad (1)$$

Where M_{PS} and M_{MWNT} present the weight of PS and MWNTs in the mixture, respectively. Eight different mixtures were prepared with 0, 1.5, 3, 5, 10, 15, 25, and 40 wt% MWNT by using this relation. Each mixture was stirred for 1 h followed by sonication for 30 min at room temperature. By placing the same number of drops on a glass plates with similar surface areas (0.8×2.5 cm^2) and allowing the water to evaporate at 60°C in the oven, dry films were obtained. After drying, samples were separately annealed above T_g of PS for 10 min at temperature 170 °C. The temperature was maintained within ±2 °C during annealing. After annealing step, films were removed from the oven and cooled down to room temperature. Figure 2 shows SEM micrographs of composite films with 15 and 40 wt%MWNT content before and after annealing at 170 °C, respectively. After annealing treatment, SEM images clearly presents the coalescence of PS particles. The shapes of PS particles are destroyed and the microstructure of the latex has been disappeared completely. The thickness of the films was determined from the weight and the density of samples and ranges from 2.4 to 5.4 μm.

Fluorescence Measurements

Fluorescence measurements were carried out using a Perkin Elmer Model LS-50 fluorescence spectrophotometer. Before fluorescence experiments, composite films were placed in a round quartz tube (4.0cmx1.0cmx1.0 cm) and the tube was flushed with nitrogen until all of the oxygen was removed from the film (Fig. 3a). Then, the quartz tube was placed in spectrophotometer and films were illuminated with the 345 nm excitation light of P. O2 diffusion experiments were performed for each film sample at room temperature (24 °C) and in all experiments maximum peak at 395 nm were used for the pyrene intensity (I_P) measurements. When these films are exposed to air, oxygen molecules penetrates into the films and the excited state of many pyrenes is rapidly quenched when encountering an oxygen molecule. The key parameter for understanding the response of the system to the presence of oxygen, assuming diffusion controlled quenching, is the intensity of unquenched pyrenes. Thus, we monitor the fluorescence emission intensity of P molecules to get information

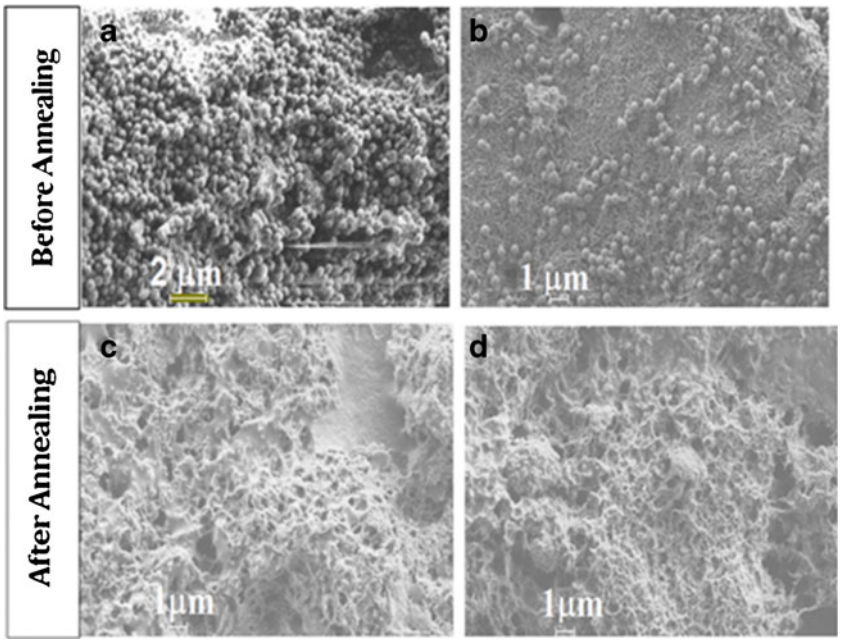

Fig. 2 SEM pictures of composite films prepared with 15 and 40 wt% MWNT content before annealing (**a, b**) and after annealing at 170 °C (**c, d**), respectively

about the diffusion of oxygen into the film. The change in pyrene intensity, I_P was monitored against time, after the quartz tube was open to the air for (O2) diffusion experiments by using time-drive mode of spectrophotometer (Fig. 3b). All measurements were made at the 90° position and the slit widths were kept at 8 nm. Since the diffusion measurements required that oxygen permeate only one surface of the film, a small region in the center of the films was masked off for measurement using black tape on the opposite side of the window from the samples. This was also done to prevent reflection of light.

Theoritical Considerations

Fluorescence Quenching by Oxygen

The mechanism of oxygen quenching involves a sequence of spin allowed internal conversion processes which take place within a weakly associated encounter complex between the probe and oxygen. The product is either a singlet ground state or an excited triplet species [29]. Data generated from oxygen quenching studies on fluorescence molecules in homogeneous medium are usually analyzed using the Stern-Volmer relation (Eq. 1), provided that the oxygen concentration $[O_2]$ is not too high [30].

$$\frac{I_0}{I} = 1 + k_q \tau_0 [O_2] \tag{1a}$$

In this equation, I and I_0 are, respectively, the fluorescence intensities in the presence and absence of oxygen, k_q is the bimolecular quenching rate constant and τ_0 is the fluorescence lifetime in the absence of O_2. This equation requires that the decay of fluorescence is single exponential and, moreover, that quenching interactions occur with a

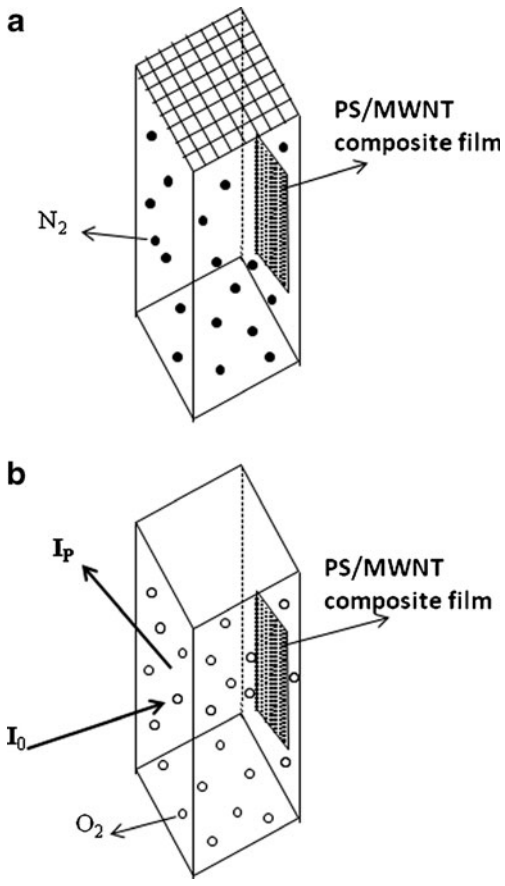

Fig. 3 Diffusion cell in the PerkinElmer LS-50 spectrofluorimeter: **a** Diffusion cell filled with nitrogen, **b** Diffusion cell exposed to air for oxygen diffusion. I_0 and I_P are the excitation and emission intensities at 345 and 395 nm, respectively

unique rate constant, k_q. From the slope of a plot of I_0/I versus $[O_2]$, k_q can be determined provided that τ_0 is known.

In this equation, I and I_0 are the fluorescence intensities in the presence and absence of oxygen, respectively, k_q is the bimolecular quenching rate constant and τ_0 is the fluorescence lifetime in the absence of O_2. This equation requires that the decay of fluorescence is single exponential and, moreover, that quenching interactions occur with a unique rate constant k_q. From the slope of a plot of I_0/I versus $[O_2]$, k_q can be determined provided that τ_0 is known. Diffusion coefficients related to the quenching events can be calculated from the time-independent Smoluchowski-Einstein [30] equation,

$$k_q = \frac{4\pi N_A (D_P + D_q) pR}{1000} \tag{1b}$$

Where D_P and D_q are diffusion coefficients of the excited probe and quencher, respectively, p is the quenching probability per collision, R is the sum of the collision radii ($R_P + R_q$), and N_A is Avogadro's number. Eqs. (1a) and (1b) can also be applied to the case of quenching of polymer-bound excited states in glass as long as the fluorescence decay is exponential and k_q is single-valued. A simplifying factor in the interpretation of k_q is the general assumption that $D_P << D_q$ when the probe is covalently attached to a polymer. For quenchers as small as molecular oxygen, such an assumption would not be unwarranted. On the time scale of fluorescence the overall translational diffusion coefficient of the polymer coil is usually not important; the relevant diffusion coefficient is that for motion of individual chain segments.

Diffusion in Plane Sheet

Fick's second law of diffusion was used to model diffusion phenomena in plane sheet. The following equation is obtained by assuming a constant diffusion coefficient, for concentration changes in time [31]

$$\frac{C}{C_0} = \frac{x}{d} + \frac{2}{\pi}\sum_{n=1}^{\infty}\frac{\cos n\pi}{n}\sin\frac{n\pi x}{d}\exp\left(-\frac{Dn^2\pi^2 t}{d^2}\right) \tag{2}$$

Where d is the thickness of the slab, D is the diffusion coefficient of the diffusant, and C_0 and C are the concentration of the diffusant at time zero and t, respectively. x corresponds to the distance at which C is measured. We can replace the concentration terms directly with the amount of diffusant, M, by using the following relation:

$$M = \int_v CdV \tag{3}$$

When Eq. 3 is considered for a volume element in the plane sheet and substituted in Eq. 2, the following solution is obtained [31]:

$$\frac{M_t}{M_\infty} = 1 - \frac{8}{\pi^2}\sum_{n=0}^{\infty}\frac{1}{(2n+1)^2}\exp\left(-\frac{D(2n+1)^2\pi^2 t}{d^2}\right) \tag{4}$$

Here M_t and M_∞ represent the amounts of diffusant entering the plane sheet at time t and infinity, respectively.

Results and Discussion

In Fig. 4, normalized pyrene intensity, I_p curves are presented against diffusion time for films having different MWNT content exposed to oxygen. It is seen that, for all film samples, oxygen diffusion began as soon as the films are exposed to air. As oxygen diffused through the planar film, the emission intensity of the pyrene decreased according to Eq. 1 for each MWNT content film and was saturated once oxygen equilibrated in the film. Here, it has to be noted that the quenching rate for low MWNT content film is lower than for high MWNT content film predicting the more rapid quenching of excited pyrenes by O_2 molecules diffused into the high MWNT content composite films. All curves behave almost in the same fashion, as oxygen diffused through and equilibrated in the film. It is also seen that the diffusion curves reach their equilibrium value at shorter times for higher MWNT content films.

In order to interpret the above findings, Eq. 1 can be used by expanding in a series for low quenching efficiency, i. e. $k_q\tau_0[O_2] << 1$ which then produces the following useful result:

$$I \approx I_0\left(1 - k_q\tau_0[O_2]\right) \tag{5}$$

During O_2 diffusion into the latex films, P molecules are quenched in the volume which is occupied by O_2 molecules

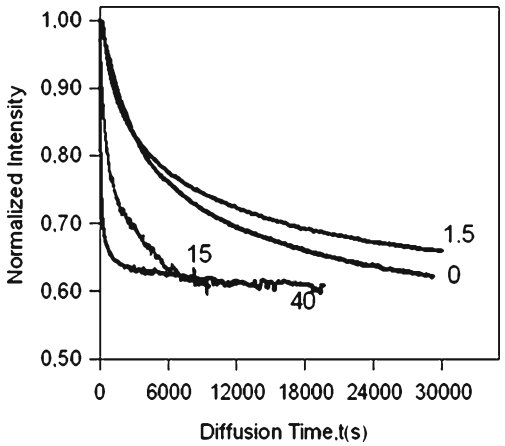

Fig. 4 The time behavior of pyrene, P, fluorescence intensity, I_P, during oxygen diffusion into the composite films with different MWNT content. Numbers on each curve indicates the MWNT content (%) in the film

at time, t. Then P intensity at time t can be represented by the volume integration of Eq. 5 as

$$I_t = \frac{\int Idv}{\int dv} = I_0 - \frac{k_q \tau_0 I_0}{V} \int dv[O_2] \quad (6)$$

Where dv and V are the differential and total volume of composite film presented in Fig. 5. Here, we assume that O_2 diffusion occur in an essentially infinite bath of air. Performing the integration the following relation is obtained

$$I_t = I_0\left(1 - k_q \frac{\tau_0}{V} O_2(t)\right) \quad (7)$$

Where $O_2(t) = \int dv[O_2]$ is the amount of oxygen molecules diffuse into the film at time t. For a film on an impermeable substrate, the oxygen concentration in a layer at distance x away from the gas-film interface at time t (see Fig. 5) is given by Eq. 4. Within a thin layer, the oxygen concentration is effectively constant. Thus, combining Eq. 7 with the Fick's law (Eq. 4), the fluorescence intensity change due to change in oxygen concentration is related to the time. If it is assumed that O_2(t) corresponds to M_t then Eq. 4 can be combined for oxygen with Eq. 7 and the emission intensity from the entire film at time t is given by the integration of Eq. 7 over the layers in the film which gives the following useful relation

$$\frac{I_p}{I_0} = A + \frac{8C}{\pi^2} \exp\left(-\frac{D\pi^2 t}{d^2}\right) \quad (8)$$

Where d is now present as the film thickness, D is the oxygen diffusion coefficient, $C = \frac{k_q \tau_0 O_2(\infty)}{V}$ and $A = 1 - C$. Here $O_2(\infty)$ is the amount of oxygen molecules diffused into the film at time infinity. Now, this expression can be used to interpret the diffusion curves in Fig. 4. Here, by flushing the cell with nitrogen, the oxygen concentration was assumed to be zero both inside and outside of the film. Hence, the P intensity is assumed to be maximum (=I_0) at the beginning. When the film was exposed to air at time zero, while the O_2 concentration increases to its final uniform equilibrium value inside the film, emission intensity decreases to its minimum equilibrium value. As a result, we combined the linear Stern-Volmer equation with the diffusion model to extract the diffusion coefficients from the experimental data. The logarithmic form of Eq. 8 can be written as follows:

$$Ln\left(\frac{Ip}{I_0} - A\right) = Ln\left(\frac{8C}{\pi^2}\right) - \frac{D\pi^2}{d^2} t \quad (9)$$

Where $C = \frac{k_q \tau_0 O_2(\infty)}{V}$ and $A = 1 - C$. Here $O_2(\infty)$ is the amount of oxygen molecules diffuse into latex film at time infinity.

This model is fitted with the experimental data using a linear least-squares fitting method to extract both k_q and diffusion coefficient (D) values. Figure 6 shows logarithmic plot of the data in Fig. 4 versus diffusion time for various MWNT content films. The solid lines represent the best fit to the diffusion model (Eq. 9). From Fig. 6, it is seen that the experimental data for PS/MWNT composites show good correlations with the Fickian Diffusion model and hence the Fickian model adequate to characterize these composites for the O_2 diffusion. Many composite materials follow Fickian diffusion kinetics, at least at low temperatures and humidities [32]. An attempt to check the Fickian model for polymer composites containing both permeable and impermeable(glass and graphite) fibre was made by Rao et al. [33, 34]. The applicability of such a model to composites based on a permeable fibre phase (jute) was verified, both under the influence of varied internal (fibre volume fraction) and external (ambient temperature) factors. Very good correlations were found between the experimental data and a modified Fickian diffusion plot.

A good fit of the experimental data to Eq. 9 confirms the applicability of a Fickian diffusion model for the material

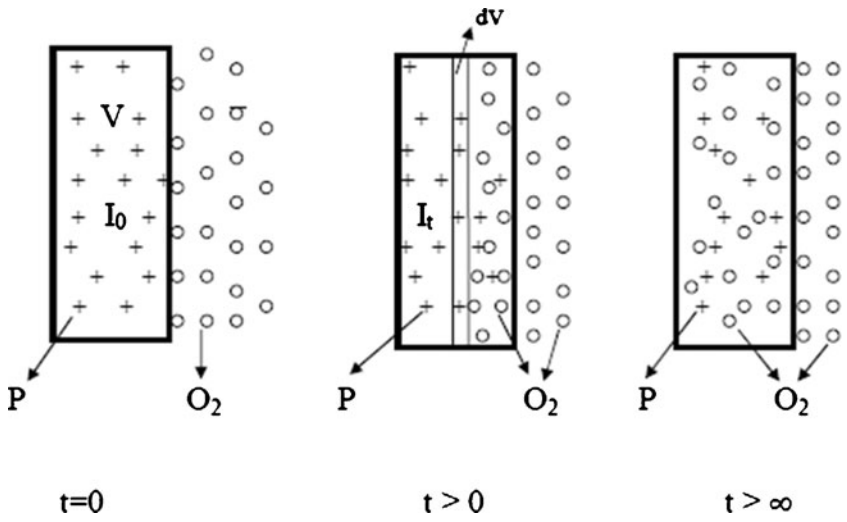

Fig. 5 Cartoon representation of oxygen diffusion into a latex film

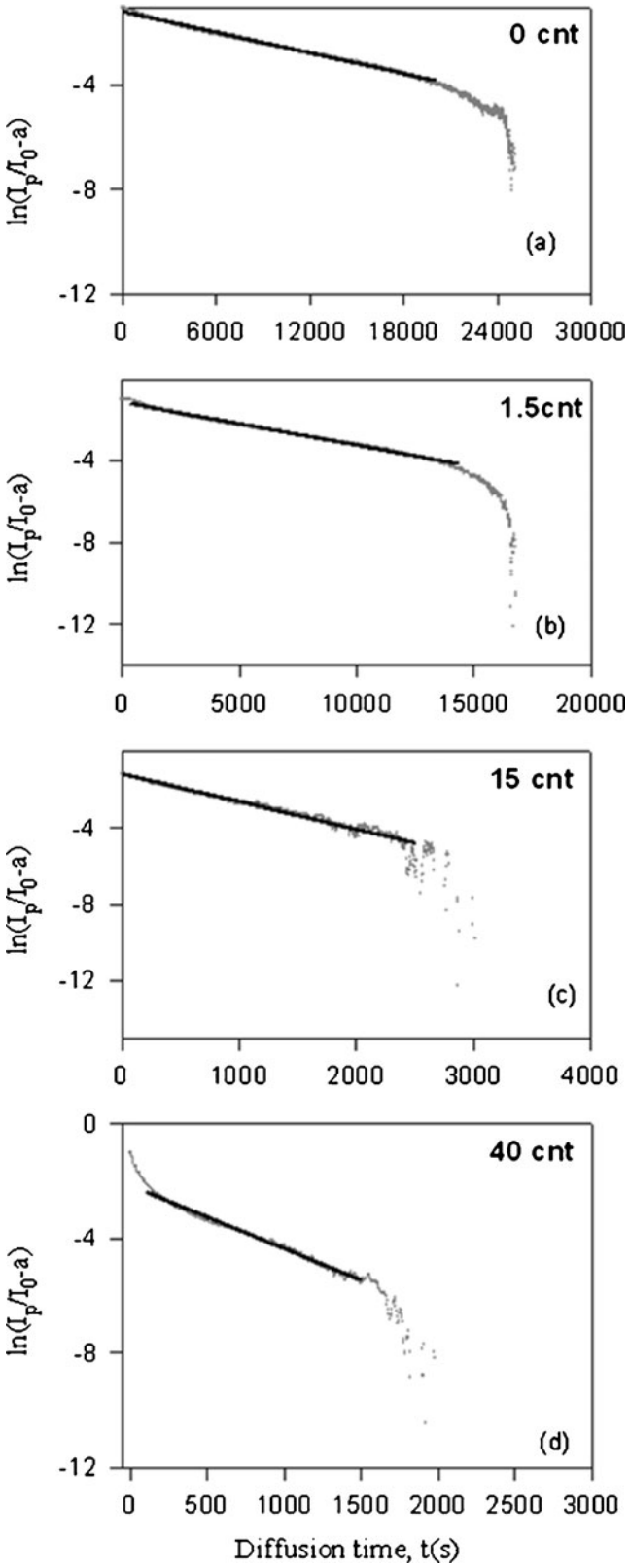

Fig. 6 Logarithmic plots of data in Fig. 1 and their fits to Eq. 9 for **a**-0, **b**-1.5 **c**-15 and **d**- 40 wt% MWNT content films

under consideration. Thus, we can extract information about both k_q and D by fitting Eq. 9 to the data in Fig. 6. Here, k_q values were calculated from C. Similar fittings were done for the all film samples and k_q and D values were produced and are listed in Table I. The diffusion coefficient is the most important parameter of the Fick`s model and shows the ability of O_2 molecules to penetrate inside the composite structures. The average D values were determined from 3 or 5 measurements on different samples in each case and the standard deviations on D values are also given in Table 1. It is seen that D coefficients are strongly dependent on MWNT content in the film. Increasing the MWNT content also increases the D values. As seen in Fig. 1, the structure of PS particles is spherical, while MWNT is long and cylindrical in structure. This difference in the formation of defects or voids in the films enhances the diffusion rate of oxygen along the film by increasing the surface area against the oxygen molecules. This result is consistent with microstructural analysis. SEM micrographs of composite films with 15 and 40 wt% MWNT content in Fig. 2 also confirm this picture. Before annealing, no deformation in PS particles is observed and PS particles keep their original spherical shapes for both samples. After annealing treatment at 170 °C, SEM images show that complete particle coalescence has been achieved. It can be clearly seen that the composite film consists of a network of bundles, especially in the 40 wt% MWNT content film, and indicates significant porosity. As shown in Fig. 2, carbon nanotubes are not well distributed in the polymer matrix and voids between the carbon nano-particles and polymer matrix appeared allowing oxygen molecules to move rapidly. Therefore, O_2 molecules can easily pass through these voids. Thus, the permeability of O_2 gas is increased, yielding high diffusion coefficients. As a result, more rapid diffusion of oxygen [27] into the higher MWNT content films occurs due to the presence of a large number of microvoids in these films. Many authors report higher loadings of CNTs in a composite do not perform as well as lower loadings [35, 36] suggesting an increase in voids or other defects as the loading of

Table 1 Experimentally obtained film thickness, diffusion coefficient (D), diffusion rate constant k_q and mutual diffusion (D_m) coefficients

MWNT (wt %)	d (μm)	$D\times10^{-12}$ ($cm^2.s^{-1}$)	$k_q\times10^{10}$ ($M^{-1}.s^{-1}$)	$D_m\times10^{-5}$ ($cm^2.s^{-1}$)
0	2.38	1.1±0.06	0.79±0.04	1.58
1.5	2.81	1.6±0.05	0.55±0.03	1.21
3	4.16	9.3±0.47	0.64±0.05	1.41
5	5.45	32.8±0.2	0.30±0.09	0.66
10	4.76	28.5±2.2	0.32±0.01	0.70
15	3.38	19.7±1.6	0.50±0.01	1.10
40	4.08	41.3±2.9	0.77±0.12	1.69

CNTs increases, likely due to the difficulty of homogeneously dispersing concentrated CNT/polymer melts or solutions. Lim et al. [37] studied MD simulations of solubilities and self-diffusivities of CO_2 and CH_4 in amorphous PEI and PEI-SWCNT matrix. They found that, self-diffusivities of the gases in the polymer composites are much larger than those in pure PEI. They explained this result as a squeezing effect of the nanotubes on the polymer matrix that changes the composite polymers' free-volume distributions and makes them more sharply peaked. The presence of nanotubes also creates several cavities with large volumes that give rise to larger diffusivities in the polymer composites. This effect is due to the repulsive interactions between the polymer and the nanotubes in consistent with our findings.

These results are also consistent with previous studies [38–41]. Generally, enhancement in the gas permeability of polymers by putting inorganic fillers into the organic polymer resulted from the disturbed polymer chain packing by the nanofillers [38]. Therefore, the well dispersed state of carbon nanotubes and their good adherence effectively increases gas permeability as the result of effective insertions between the polymer chains of the matrix. It was reported that addition of 2 wt% of modified carbon nanotubes loading to the polyethersulfone resulted in about 19.97 % increases in the permeability of CO_2, while the permeability of CH_4 increased up to 33.79 %. However, for small gas molecules, such as CO_2, the permeability increased slightly with the addition of carbon nanotubes in the polyethersulfone (PES) host matrix. The main pathways of gas transport through the mixed matrix membranes are through the dense layer of the PES matrix, highly selective carbon nanotubes and non-selective gaps or voids between the matrix and sieve particles. It was observed that the main factor affecting the increase of CH_4 permeability with the addition of carbon nanotubes into the polymer host resulted from the extremely rapid diffusion of gas molecules adsorbed inside the carbon nanotubes. FESEM data also showed that the carbon nanotubes are well dispersed in the polymer matrix and serve as channels to transport gas molecules [39–41]. It is known that the addition of filler into polymer films above a critical percentage creates voids [42, 43] in the polymer matrix. Ponomarev and Gouterman [42] have reported that the addition of high amounts of titanium oxide (TiO_2) in pressure sensitive (PSP) paints cause the presence of a large fraction of microvoids inside the films. As a result, air can diffuse very rapidly to the inside of the coating through these voids.

On the other hand, although all diffusion curves in Fig. 4 follow Fickian diffusion model, the logarithmic plot of diffusion curve for 40 wt% MWNT content film (see Fig. 6) represents two different regimes at short and longer times. The linear curve at longer times obeys the Fickian model. However, the non-linear curve at short times represent non-Fickian behavior. Here, we assume that the PS polymer is the continous phase and the film thickness is uniform. From the results, it is understood that up to acertain MWNT content, MWNT particles disperse almost uniformly throughout the film and the film surfaces can be regarded almost smooth. Thus the assumption of uniform film thickness works and O_2 molecules obey Fickian diffusion kinetics. But, at high MWNT contents, as can also be seen from SEM images in Fig. 2, a lot of voids or defects appear in the films likely due to the difficulty to disperse MWNT homogeneously. As a result, the film thickness is not uniform and film surfaces are not smooth. Due to this non-uniform film thickness, the diffusion behavior of O_2 deviates from the Fickian kinetics at the beginning of the diffusion process showing a non-Fickian behavior as in the case 40 wt% MWNT content film.

When the pyrene diffusion in the latex film is omitted and $p=1$ is taken then Eq. 1b becomes as

$$k_q = \frac{4\pi N_A D_m R}{1000} \tag{10}$$

Here D_m is called as mutual diffusion coefficient which can now be assumed to be the self diffusion coefficient of O_2 in the composite film. Since k_q is known and if ***R*** is taken as the radius of pyrene [37] then the averaged D_m values are found and listed in Table I for the composite films having different MWNT content. It is seen in Table I that D_m is independent of MWNT content in composite films i.e. once O_2 penetrates into the film then it moves in short range independent of the material structure. D_m value obtained in the present study ($10^{-5}cm^2.s^{-1}$) is one order larger than that previously obtained ($10^{-6}cm^2.s^{-1}$) by using the same technique [26, 27, 44]. This shows that the voids in composite films helps the rapid quenching of excited pyrene molecules and reduce their response time.

Conclusion

We have presented a simple, fast, and practical route to measure the diffusion of oxygen into PS/MWNT composite films for different MWNT contents using a combination of fluorescence quenching method and Fickian transport. Diffusion experiments demonstrated that the quenching rate during oxygen diffusion was completely consistent with Fickian diffusion, even in the presence of high (40 wt%) MWNT content. The diffusion coefficients increased drastically with increase of MWNT content and this increase was explained via the existence of large amounts of pores in composite films which facilitate oxygen penetration into the structure. The results showed that MWNT has presented serious effects on the permeation properties of the composite

matrix. On the other hand, results suggest that self diffusion of oxygen molecules in the composite films are not affected by the size and the structure of the composite films. In other words, D_m values give information only on local environment. Here one can also argue that O_2 molecules can also penetrate through the interior part of MWNT, which may contribute to the larger D values producing higher permeability of the composite films.

References

1. Vara RA, Jandt KD, Kramer EJ, Giannelis FP (1996) Microstructural evolution of melt intercalated polymer-organically modified layered silicates nanocomposites. Chem Mater 8:2628
2. Noh MW, Lee DC (1999) Synthesis and characterization of PS-clay nanocomposite by emulsion polymerization. Polym Bull 42:619
3. Friedlander HZ, Grink CR (1964) Synthesis, thermal properties and applications of polymer-clay nanocomposites. J Polym Sci Polym Lett 2:475–479
4. Kato C, Kuroda K, Takahara H (1981) Preparation and electrical-properties and of quaternary ammonium montromorillonite-polystrene complexes. Clay Clay Miner 29:294
5. Doh JG, Cho I (1998) Synthesis and properties of polystyrene organoammonium montmorillonite hybrid. Polym Bull 41:511
6. Li Y, Zhao B, Xie SB, Zhang S (2003) Synthesis and properties of poly(methyl methacrylate)/montmorillonite (PMMA/MMT) nanocomposites. Polym Int 52:892
7. Goldoni A, Larciprete R, Petaccia L, Lizzit S (2003) Single-wall carbon nanotube interaction with gases: sample contaminants and environmental monitoring. J Am Chem Soc 125:11329–11333
8. Pietraß T, Dewald JL, Clewett CFM, Tierney D, Ellis AV, Dias S, Alvarado A, Sandoval L, Tai S, Curran SA (2006) Electron spin resonance and Raman scattering spectroscopy of multi-walled carbon nanotubes: a function of acid treatment. J Nanosci Nanotechnol 6:135–140
9. Barrer RM (1968) In: Crank J, Park GS (eds) Diffusion in polymers. Academic Press, New York, pp 164–217
10. Gorrasi G, Tammaro L, Tortora M, Vittoria V, Kaempfer D, Reichert P, Mülhaupt R (2003) Transport properties of organic vapors in nanocomposites of isotactic polypropylene. J Polym Sci Pol Phys 15:1798
11. Lu X, Manners I, Winnik MA (2001) Polymer/silica composite films as luminescent oxygen sensors. Macromolecules 34:1917
12. Bharadwaj RK (2001) Modeling the barrier properties of polymer-layered silicate nanocomposites. Macromolecules 34:9189
13. Villaluenga PG, Khayet M, Lopez-Manchado MA, Valentin JL, Seoane B, Mengual JI (2007) Gas transport properties of polypropylene/clay composite membranes. Eur Polym J 43(4):1132
14. Gorrasi G, Tortora M, Vittoria V, Kaempfer D, Mülhaupt R (2003) Transport properties of organic vapors in nanocomposites of organophilic layered silicate and syndiotactic polypropylene. Polymer 44:3679
15. Wen WY (1993) Motion of sorbed gases in polymers. Chem Soc Rev 22:117
16. Cox ME, Dunn B (1986) Oxygen diffusion in poly (dimethyl siloxane) using fluorescence quenching .2. Filled samples. J Polym Sci Pol Chem 24:621
17. Shaw G (1967) Quenching by oxygen diffusion of phosphorescence emission of aromatic molecules in polymethyl methacrylate. Trans Faraday Soc 63:2181
18. Barker RE (1962) Diffusion in polymers: optical techniques. J Polym Sci 58:553
19. Mac Callum JR, Rudkin AL (1978) A novel technique for measuring TH diffusion constant of oxygen in polymer films. Eur Polym J 14:655
20. Cox ME, Dunn B (1986) Oxygen diffusion in poly (dimethyl siloxane) using fluorescence quenching. 1. Measurement technique and analysis. J Polym Sci 24:621–636
21. Cox ME, Dunn B (1986) Oxygen diffusion in poly (dımethyl sıloxane) using fluorescence quenching. 2. Filled Samples. J Polym Sci 24:2395–2400
22. MacCallum JR, Rudkin AL (1978) A novel technique for measuring TH diffusion constant of oxygen in polymer films. Eur Polym J 14:655–656
23. Lu X, Manners I, Winnik MA (2001) In: Valuer B, Brochan JC (eds) Fluorescence spectroscopy; New trends in fluorescence spectroscopy. Springer Verlag, New York, ch. 12:229
24. Jayarajah CN, Yekta A, Manners I, Winnik MA (2000) Oxygen diffusion and permeability in alkylaminothionylphosphazene films intended for phosphorescence barometry applications. Macromolecules 33(15):5693
25. Ruffolo R, Evans C, Liu XH, Ni Y, Pang Z, Park P, MacWilliams A, Gu X, Lu X, Yekta A, Winnik MA, Manners I (2000) Phosphorescent oxygen sensors utilizing sulfur-nitrogen-phosphorus polymer matrixes: synthesis, characterization, and evaluation of poly(thionylphosphazene)-b-poly(tetrahydrofuran) block copolymers. Anal Chem 72:1894
26. Pekcan O, Ugur S (1999) Oxygen diffusion into latex films annealed at various temperatures: a fluorescence study. J Coll Interface Sci 217:154–159
27. Pekcan O, Ugur S (2000) Packing effect on oxygen diffusion in latex films; a photon transmission and fluorescence study. Polymer 41:7531–7538
28. Liu JS, Feng JF, Winnik MA (1994) Study of polymer diffusion across the interface in latex films through direct energy transfer experiments. J Chem Phys 101:9096
29. Birks JB (1975) Organic molecular photophysics. Wiley-Interscience, New York
30. Rice SA (1985) In: Bamford CH, Tipper CFH, Compton RG (eds) Diffusion-limited reactions in comprehensive chemical kinetics. Elsevier, Amsterdam
31. Crank J (1970) The mathematics of diffusion. Oxford University Press, London
32. Matthews FL, Rawlings RD (2003) Composite materials: engineering and science. Woodhead publishing limited, Cambridge-England
33. Rao RMVGK, Balasubramanian N, Chanda M (1981) Moisture absorption phenomenon in permeable fiber polymer composites. J Appl Polymer Sci 26:4069
34. Rao RMVGK, Chanda M, Balasubramanian (1983) N "a fickian diffusion model for permeable polymer composites. J Reinf Plast Compos 2:289–299
35. Weisenberger MC, Grulke EA, Jacques D, Rantell T, Andrews R (2003) Enhanced mechanical properties of polyacrylonitrile/multiwall carbon nanotube composite fibers. J Nanosci Nanotech 3(6)
36. Zeng J, Saltysiak B, Johnson WS, Schiraldi DA, Kumar S. Processing and properties of poly(methyl methacrylate)/carbon nano fiber composites. Composites Part B: Eng
37. Lim SY, Sahimi M, Tsotsis TT, Kim N (2007) Molecular dynamics simulation of diffusion of gases in a carbon-nanotube–polymer composite. Phys Rev E 76:011810
38. Vu DQ, Koros WJ, Miller SJ (2003) Mixed matrix membranes using carbon molecular sieves - I. Preparation and experimental results. J Membr Sci 211:311
39. Chen H, Sholl DS (2006) Predictions of selectivity and flux for CH4/H-2 separations using single walled carbon nanotubes as membranes. J Membr Sci 269:152

40. Ma PC, Kim JK, Tang BZ (2006) Functionalization of carbon nanotubes using a silane coupling agent. Carbon 44:3232
41. Delozier DM, Watson KA, Smith JG, JrTC C, Connel JW (2006) Investigation of aromatic/aliphatic polyimides as dispersants for single wall carbon nanotubes. Macromolecules 39:1731
42. Ponomarev S and Gouterman M (1998) presented at the 6th annual pressure sensitive paint workshop, settle, WA, Act. 6–8
43. Kneas AK, Demas JN, Nguyen B, Lockhart A, Xu W, DeGraff BA (2002) Method for measuring oxygen diffusion coefficients of polymer films by luminescence quenching. Anal Chem 74:1111
44. Ugur S, Yargi O, Pekcan O (2009) Oxygen diffusion into polystyrene-bentonite films. Appl Clay Sci 43:447–452